Charge Transfer and Solvation of Betaine-30 in Polar SolventsA Femtosecond Broadband Transient Absorption Study

ARTICLE *in* THE JOURNAL OF PHYSICAL CHEMISTRY A · MAY 2001

Impact Factor: 2.69 · DOI: 10.1021/jp004007e

4 AUTHORS, INCLUDING:

Sergey A Kovalenko
Humboldt-Universität zu Berlin
154 PUBLICATIONS **2,831** CITATIONS

Charge Transfer and Solvation of Betaine-30 in Polar Solvents—A Femtosecond Broadband Transient Absorption Study

S. A. Kovalenko,* N. Eilers-König, T. A. Senyushkina, and N. P. Ernsting*

Institut für Chemie, Humboldt Universität zu Berlin, Bunsenstrasse 1, D-10117 Berlin, Germany

Received: October 31, 2000; In Final Form: March 8, 2001

Betaine-30 in polar solvents was studied with the pump−supercontinuum probe technique after ca. 50 fs excitation at 532 and 634 nm. By monitoring the spectral evolution of stimulated emission, excited-state absorption, and bleaching, photoinduced solvation and ultrafast intramolecular rearrangement in the excited state are resolved for the first time. This rearrangement is related to intramolecular electron transfer (iET). In acetonitrile, the rate coefficient k of iET satisfies the condition of solvent control, $k = 1/\tau_0$ (±10%), where τ_0 is a characteristic solvent relaxation time deduced from the solvation correlation function $C(t)$. Back ET or internal conversion proceeds from a molecular conformation which differs from that in the ground state. It develops on a picosecond time scale and is followed by cooling of hot betaine molecules by the solvent. By comparing transient Stokes shift data with $C(t)$, we extract solvation and intramolecular reorganization energies associated with high and low frequency optically active modes. The solvatochromism of betaine-30 contains substantial solvent-dependent intramolecular contributions and, therefore, cannot be understood without accounting for internal degrees of freedom.

I. Introduction

The pyridinium *N*-phenolate dye betaine-30 (Scheme 1) is one of the most sensitive solvatochromic probes known today. It has been used for polarity measurements of more than 300 pure solvents and of many solvent mixtures.[1,2] Betaine-30 exhibits negative solvatochromism which results from a dramatic reduction of the dipole moment upon photoexcitation.[3] When going from diphenyl ether to water solutions, the absorption band shifts to the blue from 810−450 nm by ≈10 000 cm.$^{-1}$ Figure 1 shows this behavior for the solvents relevant in this study. Fluorescence from the first excited state has never been observed, indicating rapid $S_1 \rightarrow S_0$ internal conversion, i.e., back electron transfer (bET) to the ground state, or other relaxation processes in the S_1 state.

Most of the experimental results on the excited-state dynamics of betaine-30 were reported by Barbara's group.[4−6] Since then, only a few experiments have been published,[7] among them a resonance Raman study by Zong and McHale[8] and picosecond anti-Stokes Raman measurements by Hogiu et al.[9,10] Barbara and co-workers measured transient absorption to derive the rate of internal conversion in a number of solvents at various temperatures. Fluorescence was not yet resolved in these experiments. The authors tried to rationalize their data with a modified Marcus theory[11,12] for bET in the inverted region.[4,13,14] The theory requires the knowledge of intramolecular and solvation reorganization energies. Being not available from direct measurements, they were estimated from absorption band shape analysis.[4,15] Later on, other experimental[8] and theoretical[16−19] estimates of these energies appeared. They show little agreement[19] ranging, for example, for solvation in acetonitrile, from 800 to 6000 cm^{-1}.

SCHEME 1

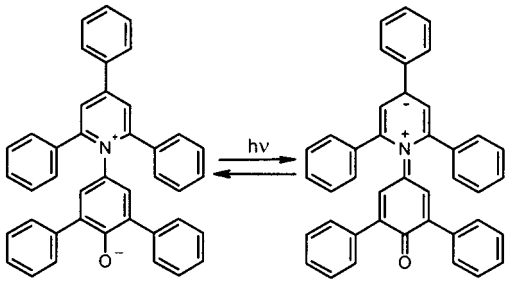

The above theories[4,13,14] of bET implicitly assume rigidity of the solute in the excited state. More precisely it is supposed that intramolecular rearrangements do not affect the spectral evolution; only in this case may the rate of bET be related in a simple way to steady-state properties such as absorption and fluorescence spectra and Raman excitation profiles.[20] Contrary to this assumption, recent theoretical calculations[18,19,21−23] on betaine-30 predict high sensitivity of the absorption spectrum to conformational rearrangements, for example, a change of the central dihedral angle. At the same time, the latest (and only) molecular dynamics simulation study[18] does not show any essential dynamics in the excited state of betaine-30, thus supporting to some extent the above treatments.

The present work reports new experimental results on the excited-state dynamics of betaine-30. By using the femtosecond pump−supercontinuum probe (PSCP) technique,[24] we monitored the complete spectral evolution of the transient absorption signal. Characteristic features of this evolution suggest an ultrafast intramolecular electron transfer (iET) process in the excited state followed by much slower bET, or internal conversion. The latter proceeds from a molecular conformation which differs from that in the ground state.

* To whom correspondence should be addressed.

10.1021/jp004007e CCC: $20.00
Published on Web 05/02/2001

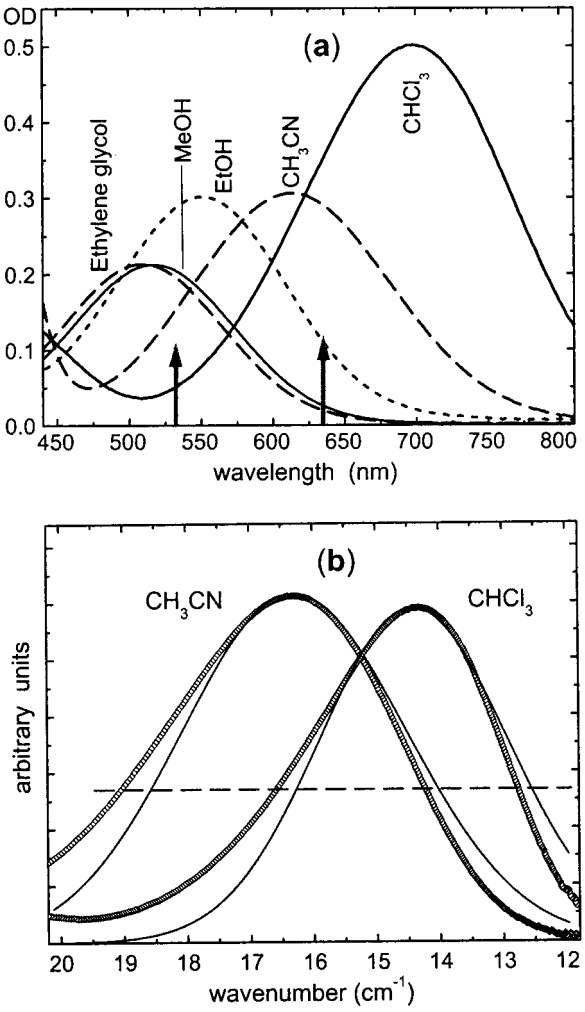

Figure 1. (a) Absorption spectra of betaine-30 (from right to left) in chloroform, acetonitrile, ethanol, methanol, and ethylene glicol. Concentration is 7.8×10^{-4} M/L. Excitation wavelengths are shown by arrows. (b) Gaussian fits of the spectra for chloroform and acetonitrile. The dashed line indicates the level of half-maximum.

II. Experiment

The experimental setup has been described elsewhere.[24−26] Betaine-30 was excited with 50 fs pulses centered at 532 nm[24,25] or with 60−80 fs pulses at 631−637 nm.[26] In the case of red excitation, the pump parameters differed in various experiments and they are given in the results section. The pump-induced transient absorption signal $\Delta OD(t,\lambda)$ was monitored with a supercontinuum probe in the spectral range of 360−770 nm or in the range of 510−930 nm, for green and red excitation, respectively. The sample net thickness was 0.3−0.4 mm. The optical density of the sample at the pump wavelength was adjusted to ≈0.6 which corresponds to a concentration of $(2\div6) \times 10^{-3}$ mol/L depending on the solvent. No concentration dependence of the absorption spectra was found in this range. The solution was flown out of the interaction region after each laser short. After passing through the sample, the supercontinuum was dispersed by a polychromator and registered on a photodiode array (512 pixels) with a spectral resolution of 1.5 nm. The recorded transient spectra were time-corrected for the chirp of the supercontinuum.[24] The time resolution after time correction and deconvolution is 20 fs for both experiments. All transient measurements were performed at ambient temperature. Stationary absorption spectra were measured with a Shimadzu spectrophotometer. Betaine-30 was purchased from Aldrich and used without further purification.

III. Experimental Results

A. Transient Spectra with Red Excitation. *Acetonitrile.* In the case of acetonitrile, the excitation pulse (637 nm, 60 fs) nearly matches the absorption maximum. Transient absorption spectra are depicted in Figure 2. The negative signal corresponds to bleach or stimulated emission (SE) and the positive to excited-state absorption (ESA). Frame a shows early spectra for pump−probe delays from −60 to +40 fs in 10 fs steps. The signal for this time interval is characterized by uniform growth. ESA with a maximum at 530 nm dominates the blue region. Broad SE is recognized in the red, for $\lambda > 700$ nm, with a peak between 750 and 800 nm. The bleach band is strongly overlapped with ESA and seen as a negative signal in the region 630−750 nm.

During the pump−probe overlap, the spectra show a pronounced Raman-like structure[24] which results from both solute and solvent contributions. The Raman signal follows the pump−probe cross-correlation, reaching its maximal contrast at zero delay. Therefore, the dynamics of a Raman peak gives an effective pump pulse duration, whereas the *simultaneous* growth and decay of these peaks in *different* spectral regions reflects the quality of the time correction. For measurements reported here, our time correction is better than ±10 fs. The two negative peaks at 784 and 745 nm are due to nonresonant Raman scattering from the CH (2940 cm^{-1}) and CN (2250 cm^{-1}) stretching modes of pure acetonitrile. The same modes give anti-Stokes absorption (positive peaks) at 536 and 553 nm, respectively. The positions of the Stokes and anti-Stokes peaks allow an independent determination of the pump wavelength which was 637 nm in the present experiment. The Raman peaks are seen to experience a red shift, indicating that the pump pulse is slightly chirped. The strong signal at the excitation wavelength is the sum of three contributions: from the ground state "hole" and from the excited state "particle"[27,28] induced by pumping and from resonance Rayleigh scattering.[27−29] Last, the broad peak at 700 nm is due to resonance Raman scattering by 1300−1400 cm^{-1} modes of betaine-30.[8−10]

The further spectral evolution from 50 to 300 fs is displayed in frame b with 50 fs steps. The SE maximum shifts to the red (by 1000 cm^{-1} between 50 and 100 fs) in agreement with solvation in acetonitrile as will be discussed. Simultaneously with the shift, the integral intensity of *SE decays rapidly*, whereas the signal due to *ESA remains nearly constant* in magnitude. Because both ESA and SE are governed by the same population in the excited state, such behavior clearly indicates a transient decrease of the oscillator strength for SE. Also, a new ESA band develops which is peaked at 780 nm. We assign this band to an excited state or form of betaine-30 which is not coupled radiatively to the ground state, i.e., a "dark" state with regard to fluorescence or stimulated emission. Such changes of optical transitions cannot be explained by solvation alone; it follows that an intramolecular process takes place at the same time. At a 300 fs delay, the transient spectrum contains four contributions: an intensive blue ESA band, the bleach band, weak SE in the red, and pronounced dark-state absorption (DSA).

Starting from 300 fs, the decay of ESA in the blue becomes apparent while the bleach band also decays. This is consistent with a decrease of the excited-state population and internal conversion to the ground state. Between 300 fs and 1 ps (frame c) this process seems to be accompanied by DSA growth which is inconsistent, but the latter can be explained by overlap with SE which continues to lose oscillator strength in addition to population decay and, therefore, decays faster than DSA and, hence, registers as apparent DSA growth. From 1 to 4 ps (frame

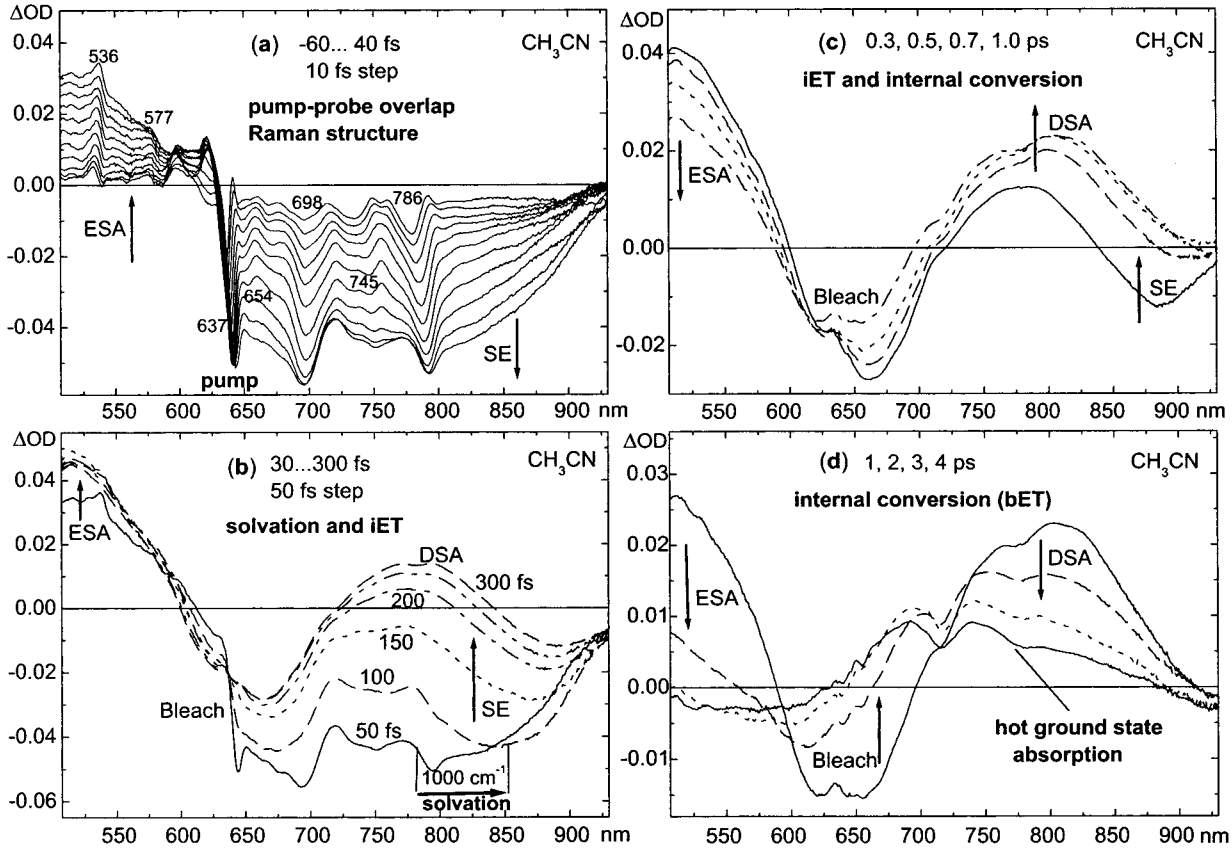

Figure 2. Transient absorption spectra of betaine-30 in acetonitrile with 637 nm excitation. Pump−probe delays and time steps are shown as inserts. Vertical arrows indicate evolution of the signal for excited-state absorption (ESA), bleach, stimulated emission (SE), and dark state absorption (DSA).

d) both ESA and DSA decay simultaneously. As the ESA vanishes, the bleach maximum shifts to 620 nm as expected from the stationary absorption spectrum. After 4 ps, the transient spectra correspond to hot absorption from the ground state.

Going back to early delays (frame a), we note that the peak of SE around 750 nm is detuned from the absorption maximum by ≈3000 cm^{-1}. This initial detuning indicates that vibrational relaxation of high-frequency modes is very fast (∼10 fs),[30−32] being not resolved in our measurements. To see this, assume that the pump pulse excites a high-frequency vibrational mode in S_1. If relaxation of this mode were slow, early stimulated emission would be peaked at the excitation frequency (which in acetonitrile corresponds to the absorption maximum and, hence, matches the largest Franck−Condon factor both for absorption and for *nonrelaxed* SE). This is however not the case in the present measurements. Therefore the initial detuning presents a direct estimate of the intramolecular reorganization energy associated with the fast modes.

Chloroform. Figure 3 displays the spectral evolution in chloroform. Now the pump pulse (634 nm, 60 fs) excites the solute at the blue side of the absorption spectrum (compare with Figure 1). The transient spectra are similar to those in acetonitrile but their evolution is much slower. The resonance Raman peak at 691 nm is less pronounced than in acetonitrile, because its intensity is related to the excess excitation energy above the 0−0 transition. The measured bleach signal, now well separated from ESA, is peaked close to the absorption maximum at 700 nm. At early delays, the ESA band has a maximum near 550 nm (frame a). As time increases, it shifts to the blue (frame c) by 1100 cm^{-1}. Stimulated emission is first seen as a red shoulder of the bleach band (frame a). At a later time, the SE band shifts to the red and decays (frame b). As in acetonitrile, the decay of SE is much faster than the decay of ESA.

Ethanol. The transient spectra in ethanol are shown Figure 4. Here the pump pulse (633 nm, 80 fs) matches the far red edge of the absorption spectrum which is now peaked at 550 nm. This has two consequences: first, the bleach band is completely hidden by ESA, and second, the bleach contribution is very weak for $\lambda > 650$ nm; therefore, the broad negative signal in Figure 4a belongs entirely to SE. The SE band is peaked at early delays around 750 nm, being detuned from the pump frequency by ≈2500 $cm.^{-1}$ Because the pump pulse excites preferentially the 0−0 transition, this detuning gives another estimate of the intramolecular reorganization energy of high-frequency modes.

B. Transient Spectra with 532 nm Excitation. These spectra are shown in Figure 5 for acetonitrile, methanol, ethanol, and ethylene glycol. Here the probe range is extended to the blue, which allows the observation of two ESA bands, with peaks at 590 nm and at 360 nm in alcohols. The first band has been already discussed. Its spectral evolution is affected by solvation (seen as a blue shift) at early delays and by overlap with hot ground state absorption at later times. The second band, ESA2 at 360 nm, is evidently much less affected by these processes. Therefore, the decay of this band gives a better estimate for the rate of internal conversion.

For ethanol solutions, one can compare the transient spectra recorded with green (Figure 5c) and red excitation (Figure 4). For example, at 100 fs, the SE band is peaked at 723 and 750 nm, respectively. The red shift of 500 cm^{-1} reflects excitation selectivity over the ground state solvent and conformational distributions, which leads to a different initial frequency for SE.

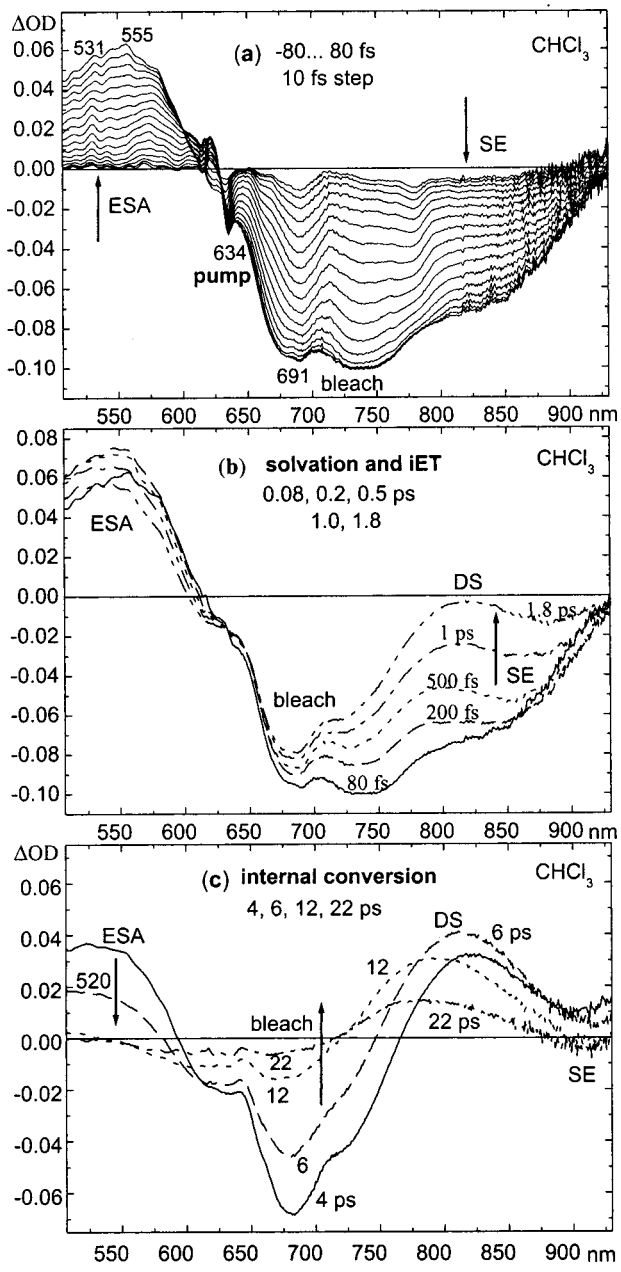

Figure 3. Same as in Figure 2 but for chloroform with 634 nm excitation.

Similarly the ESA band with red excitation is *blue* shifted relative to that with green excitation; the peaks are located at 550 and 588 nm with a difference of 1100 cm.$^{-1}$

The band peaks and widths for SE and ESA observed in our experiments together with steady-state data are collected in Table 1.

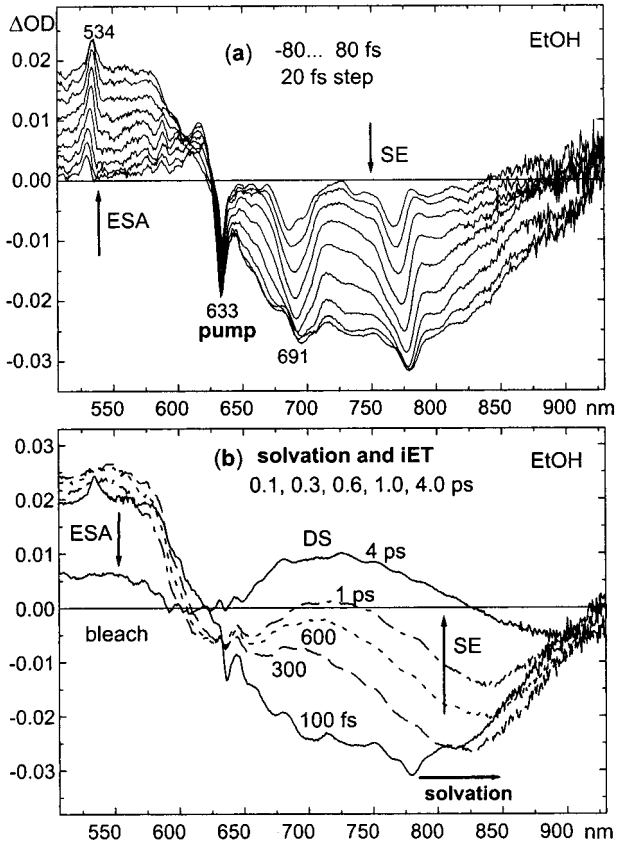

Figure 4. Same as in Figures 2 and 3 but for ethanol with 633 nm excitation.

IV. Dynamics in the Excited State

As was shown in the results section, the excited state dynamics of betaine-30 that could be resolved is characterized successively by solvation and intramolecular rearrangement or iET and by internal conversion or bET. Here we discuss these processes in more detail. A key assumption in our analysis is that at early delays iET does not disturb much the spectral evolution, which can therefore be described as pure solvation.

The solvent response to a photoinduced change of the solute dipole moment can be linked to a solvation correlation function $C(t)$ defined as[33,34]

$$C(t) = \frac{\langle \delta\Delta E(0)\delta\Delta E(t)\rangle_g}{\langle(\delta\Delta E)^2\rangle_g} \qquad (1)$$

Here $\delta\Delta$E are fluctuations of the energy gap ΔE for the $S_1 \leftarrow S_0$ transition, the subscript g refers to the equilibrated ground state, and $\langle(\delta\Delta E)^2\rangle_g$ represents the solvation contribution to the absorption bandwidth. In the linear response approximation and for an ideal solvatochromic probe, $C(t)$ can be related to transient

TABLE 1: Betaine-30: Band Peaks and Widths from Steady-State and Transient Absorption Measurements[a]

solvent	ν_A	Γ_A	$\nu_{SE}(0)$	$\Gamma_{SE}(0)$	ν_{ESA2}	Γ_{ESA2}	ν_{ESA}	Γ_{ESA}	ν_{DSA}	Γ_{DS}
acetonitrile	16 310	4450	13 450[b]	3600	27 500	5000	19 600	4500	12 380	3500
chloroform	14 330	3590	12 580[b]	2700			18 200	4500	12 270	3500
methanol	19 340	5100	14 700[c]		27 040	5000	16 900	4500		3500
ethanol	18 080	4800	14 350[c]	3800	27 500	5000	18 200	4500	13 850	3500
ethyl. glyc.	19 650	5230	14 350[c]		27 500	5000	16 900	4500		3500

[a] ν_j and Γ_j, peak frequencies and widths in cm.$^{-1}$ Subscripts denote A, $S_1 \leftarrow S_0$ absorption band; SE, stimulated emission; DSA, dark state absorption; ESA and ESA2, first and second excited-state absorption band; $\nu_{SE}(0)$ and $\Gamma_{SE}(0)$, peak and width of SE at time zero. [b] Red excitation. [c] 532 nm excitation.

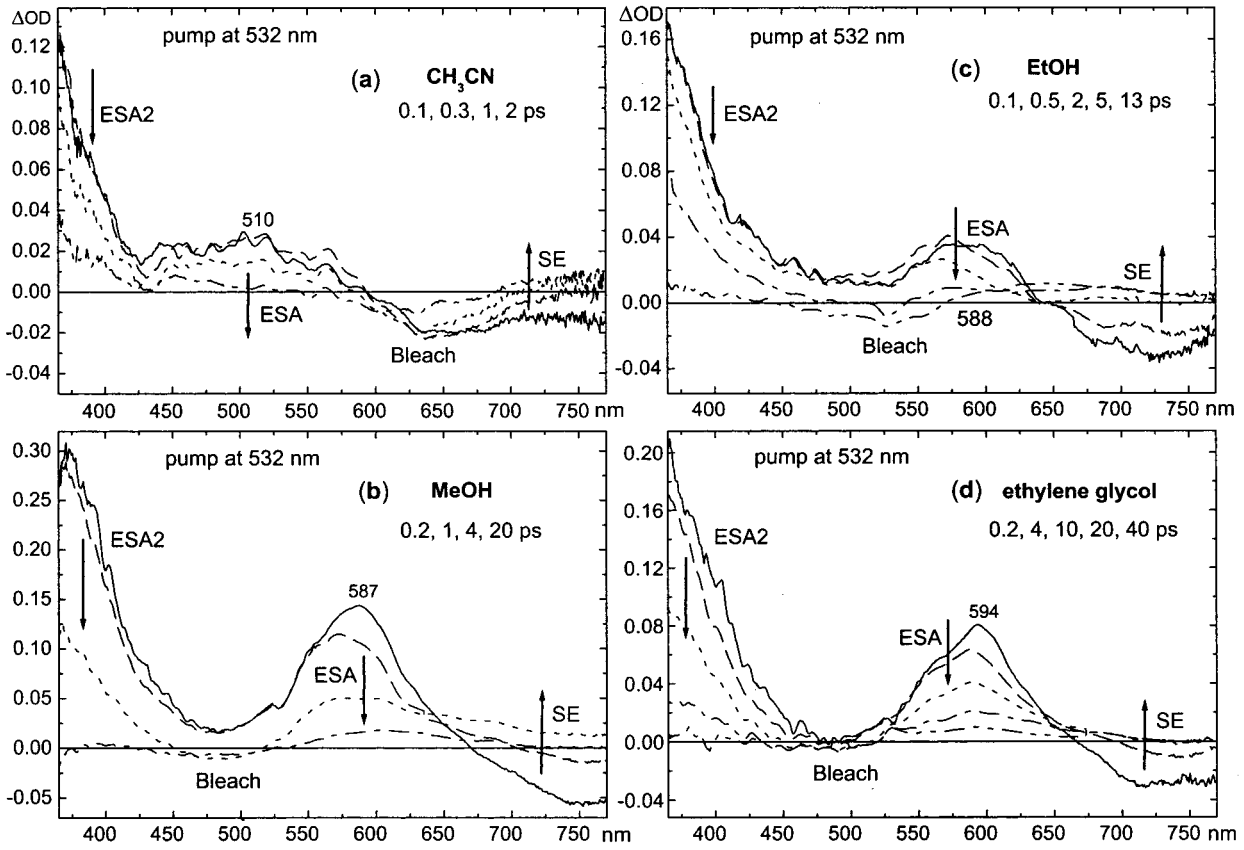

Figure 5. Transient absorption spectra of betaine-30 with 532 nm excitation in acetonitrile, methanol, ethanol, and ethylene glycol. Pump−probe delays are shown as insets. The earliest spectrum in each frame is shown as a solid line.

Stokes shift measurements[30−35]

$$C(t) = \frac{\nu_{SE}(t) - \nu_{SE}(\infty)}{\nu_{SE}(0) - \nu_{SE}(\infty)} \tag{2}$$

with $\nu_{SE}(t)$ being the peak frequency of stimulated emission at a pump−probe delay t and $\nu_{SE}(0)$ and $\nu_{SE}(\infty)$ denoting the same quantity for the time-zero and steady-state SE, respectively. Here "ideal probe" implies a solute which experiences solely solvation in the excited state. For such a probe, solvation relaxation in the excited and ground state are identical, which gives in high-temperature limit

$$\langle(\delta\Delta E)^2\rangle_g \propto kT\Delta\nu_s \tag{3}$$

where $\Delta\nu_S = \nu_{SE}(0) - \nu_{SE}(\infty)$ is the solvation Stokes shift. Thus, Stokes shift measurements allow us to evaluate $\langle(\delta\Delta E)^2\rangle_g$. Furthermore, although $C(t)$ in eqs 1 and 2 is expressed via solute−solvent parameters $\delta\Delta E$ and $\nu_{SE}(t)$, it represents in fact properties of pure solvent.[30,31,33−38] Taking C(t) from independent measurements,[30,35,36,39] we therefore rewrite eq 2 as

$$\nu_{SE}(t) = \nu_{SE}(0) + [C(t) - 1]\Delta\nu_s \tag{4}$$

Next we try to fit the experimental dependence $\nu_{SE}(t)$ with adjustable parameters $\nu_{SE}(0)$ and $\Delta\nu_S$. In so doing, we assume that the early evolution is governed by pure solvation only. These fits allow us to extract reorganization energies associated with the absorption spectrum and also to examine qualitative differences between $\nu_{SE}(t)$ and $C(t)$. The results are shown in Figure 6. Here, symbols represent the *apparent* peak positions of transient SE as given by Figures 2−5, whereas the solid curves are the corresponding fits.

Consider first acetonitrile (frame a). In this case, $C(t)$ is taken from ref 35; its representation with a Gaussian and an exponential function is given in the left column of Table 2. It is seen that the experimental points cannot be fitted simultaneously over the entire time interval of the measurement. However, it is possible to obtain a satisfactory fit at *early* delays $t < 100$ fs, when the spectral behavior is not disturbed much by intramolecular rearrangements. For acetonitrile, the fit gives $\nu_{SE}(0) = 13\,450$ cm^{-1} and $\Delta\nu_S = 4000$ cm.$^{-1}$ To give an idea about the significance of the fit, Figure 7 shows the initial region of Figure 6a enlarged with two additional curves for $\Delta\nu_S = 4800$ cm^{-1} and $\Delta\nu_S = 3200$ cm^{-1}, respectively, whereas $\nu_{SE}(0)$ was kept at 13450 cm^{-1}. From a comparison of these curves we estimate the accuracy of the extracted reorganization energies as ±12%.

The *full* fitting curve in Figure 6 displays the feasible evolution of the band gap if no intramolecular relaxation occurs at all, i.e., the evolution for an ideal solvatochromic probe. Because betaine-30 is by no means such a probe (witness the intramolecular spectral changes which were demonstrated above), its behavior in the excited-state deviates from the "predicted" one. Deviations due to iET become visible after 80 fs reaching 1400 cm^{-1} at longer delays. In fact, they are larger, of the order of 2000 cm^{-1}, because absorption from the dark state contributes to the red shift of the apparent peak of SE. The data are not corrected for such effects because at early time the latter are small. Interestingly, iET is seen to decrease the total Stokes shift which is expected from pure solvation, thus, suggesting an increase of the molecular dipole moment in the course of relaxation.

In chloroform and ethanol (frames b and c), the data can be well fitted over delays up to 1 ps as explained by slower iET in these solvents. In methanol (frame d) iET is as fast as in

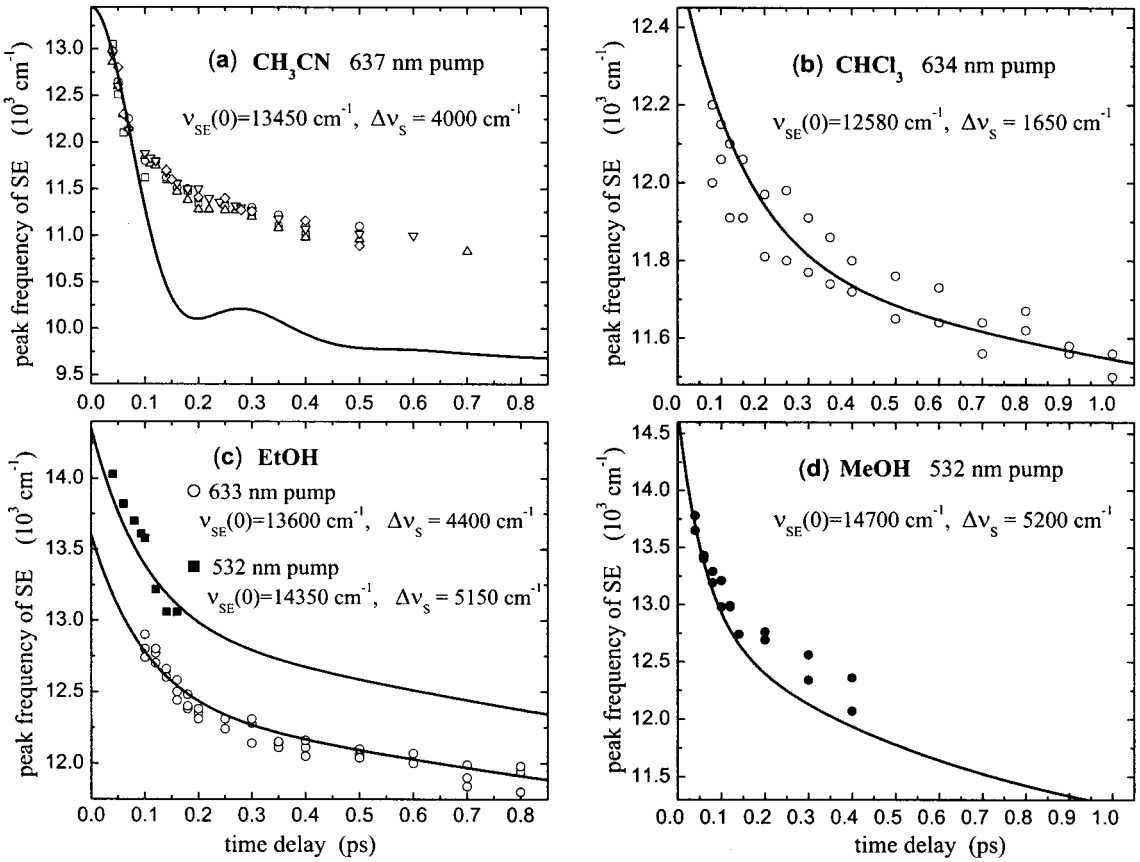

Figure 6. Transient Stokes shift of the peak of SE in acetonitrile, chloroform, ethanol, and methanol. Symbols are apparent peaks of SE from Figures 2−5; solid curves represent fits by eq 4 with the solvation correlation functions $C(t)$ from Table 1. The fitting results $\nu_{SE}(0)$ and $\Delta\nu_S$ are shown as inserts.

TABLE 2: Characteristic Times (ps) of Solvation and of Excited State ET in Betaine-30

	solvation correlation function[a] $C(t)$							iET[b] and bET[c] characteristic times					
solvent	a_{S1}	τ_{S1}	a_{S2}	τ_{S2}	a_{S3}	τ_{S3}	τ_0[d]	a_1	τ_1	a_2	τ_2	τ_{iET}[e]	τ_{bET}
acetonitrile[35]	0.67	0.065	0.33	0.60			0.092	0.70	0.07	0.30	0.33	0.092	1.2
chloroform[36,39]	0.48	0.15	0.52	3.0			0.30	0.34	0.38	0.66	2.93	0.89	5.5
methanol [39]	0.35	0.06	0.29	0.53	0.36	4.9	0.15	0.48	0.048	0.52	0.38	0.09	3.1
ethanol[39]	0.27	0.10	0.38	2.7	0.35	17	0.35					0.48	4.8
ethyl. glyc.[30]	0.31	0.19	0.26	5.0	0.44	32	0.59					2.3	9.7

[a] From references indicated in the column "solvent". $C(t)$ is fitted multiexponentially (a_{Sj} − amplitudes) except for acetonitrile, where the first component is Gaussian $\exp(-t^2/2\tau^2_{S1})$. [b] Biexponential fit. [c] Monoexponential fit. [d] $1/\tau_0 = a_{S1}/\tau_{S1} + a_{S2}/\tau_{S2} + a_{S3}/\tau_{S3}$. [e] $1/\tau_{iET} = a_1/\tau_1 + a_2/\tau_2$. The accuracy for τ_0, τ_{iET}, and τ_{bET} is ±10%.

acetonitrile; therefore, deviations start earlier. For ethanol, we make use of two sets of data, with green and red excitation. They are fitted by the same $C(t)$ but with different $\nu_{SE}(0)$ and $\Delta\nu_S$ (see inserts in frame c).

A quantitative description of iET dynamics can be obtained from band integral analysis.[40,41] The band integral BI(t;λ_1,λ_2) is defined as

$$\mathrm{BI}(t;\lambda_1,\lambda_2) = \int_{\lambda_1}^{\lambda_2} \Delta\mathrm{OD}(t,\lambda)\cdot(\mathrm{d}\lambda/\lambda) \qquad (5)$$

where (λ_1,λ_2) is the wavelength range over which the integral is taken. A remarkable property of this quantity is that it is insensitive to spectral shifts when the detection range is sufficiently broad to cover the entire spectral evolution of the band. The band integral reflects population dynamics when oscillator strengths of optical transitions do not change. Alternatively, for constant population, its change indicates changes in the oscillator strengths of relevant optical transitions. In the case of overlapping bands (such as bleach/ESA or ESA/SE), the integral remains proportional to the excited-state population and to a difference of oscillator strengths.

Figure 8a shows the evolution of the full band integral BI-(506,930) in acetonitrile. The integral was calculated in the region 506−930 nm from the transient spectra of Figure 2. The early behavior before 1 ps is shown in the insert. Open squares denote calculated points, whereas the solid curve in each frame represents a biexponential fit. The integral starts from negative values at early delays and becomes positive very fast, reaching a maximum at 1 ps. Because the ESA band in the blue does not change much during this time interval, this behavior reflects a decrease of the oscillator strength for SE and an increase of the oscillator strength for DSA which correspond to iET in the excited state. The dynamics of iET (as reflected in the full band integral) is well described by a biexponential function with τ_1 = 70 fs (70%) and τ_2 = 330 fs (30%). After 1 ps, the integral decays with 1.2 ps reflecting bET to the ground state. By 4 ps, the full band integral has decayed to 10% of its maximum, indicating that internal conversion is almost complete. However,

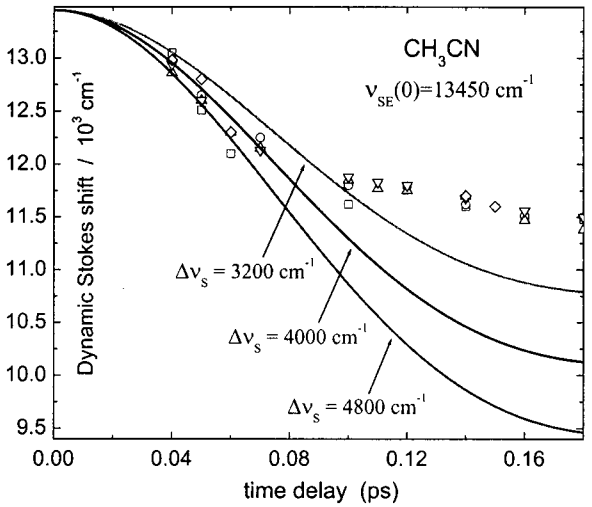

Figure 7. Same data as in Figure 6a but with the initial region enlarged. Three curves with different $\Delta\nu_S$ are plotted to show the accuracy of determining $\Delta\nu_S$.

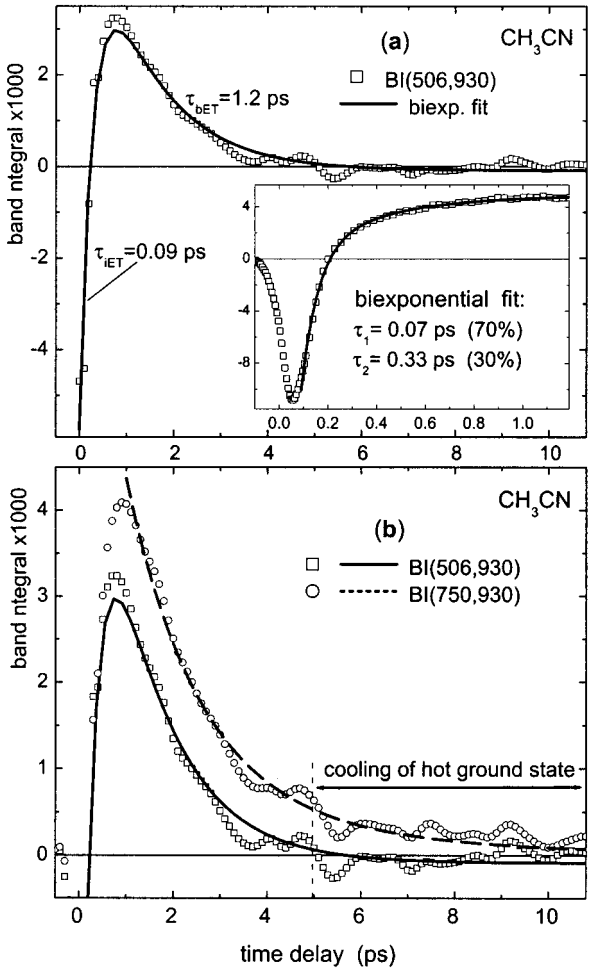

Figure 8. Dynamics of iET and of bET in acetonitrile as seen by the full band integral BI(506,930). Symbols represent experimental points and solid curves give biexponential fits. After 5 ps, the partial band integral BI(750,930) reflects cooling of the hot ground state.

the spectral evolution is not finished as seen from the behavior of the *partial* band integral BI(750,930) taken over the red tail of the absorption spectrum. The integral is shown by circles (fit by dashed line) in Figure 8b. It contains two contributions: the first comes from absorption from the dark state, and the second is due to hot ground-state absorption.[40,42] After 5 ps,

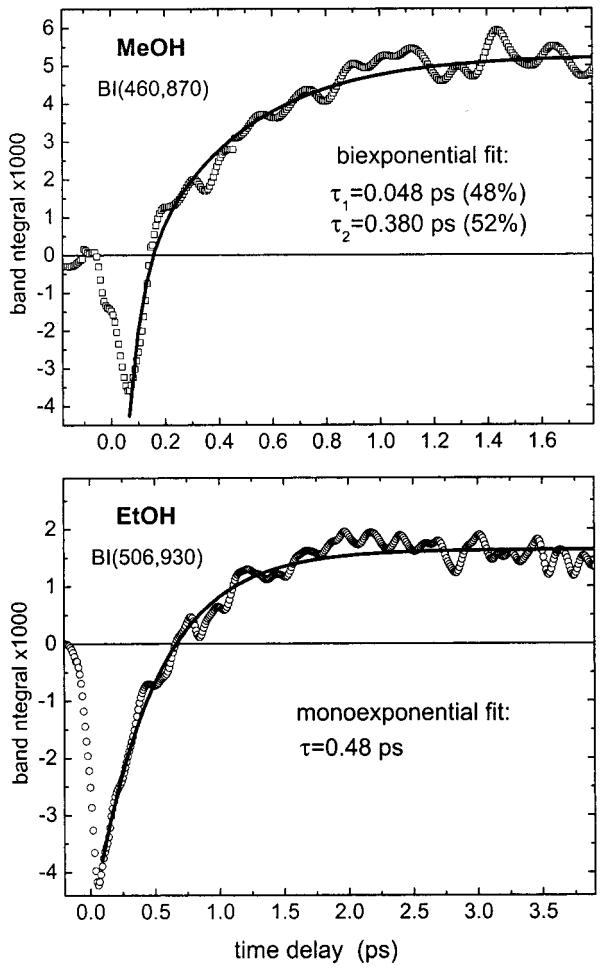

Figure 9. The same as in Figure 7 but for alcohols.

the integral describes solute−solvent energy transfer (cooling of the hot ground state) with ~3 ps characteristic time.

Figure 9 shows the behavior of the full band integral in alcohols. In methanol, iET is as fast as in acetonitrile; a biexponential fit gives $\tau_1 = 48$ fs (48%) and $\tau_2 = 380$ fs (52%). In ethanol, the dynamics is slower, with an average time constant of 480 fs.

The rate of bET can be obtained in two ways: from the long-time decay of the full band integral or from the decay of the ESA2 band. The latter case is illustrated by Figure 10, where the partial band integral BI(364,430) is taken over the ESA2 band. Symbols are experimental points calculated from the spectra of Figure 5, and solid curves represent monoexponential fits. The fits are satisfactory at longer delays but deviate from the experimental dependences at early time. For acetonitrile, the decay time of 1.15 ps is in good agreement with the 1.2 ps decay obtained from the full band integral (Figure 8a). The deviations at short times suggest that the ESA2 band is affected by iET.

Characteristic time constants and amplitudes of iET and bET together with parameters of the solvation correlation function $C(t)$ are collected in Table 2 and may now be compared. It is seen that in acetonitrile the rate of iET $1/\tau_{iET}$ is identical to the solvation rate $1/\tau_0$ (the so-called condition of solvent controlled ET). This is consistent with a view that iET itself is faster than solvation. However, because the latter creates the driving force, iET follows solvation adiabatically. In ethanol and chloroform, iET is slower than solvation, indicating that the effective driving force is relatively weak. This explains also the above-mentioned

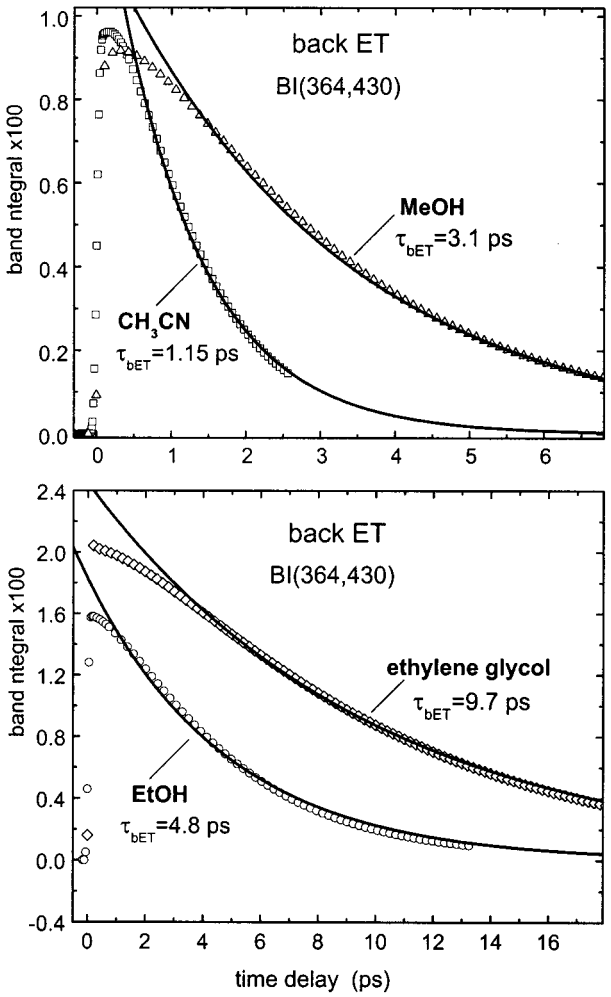

Figure 10. The dynamics of bET in acetonitrile, methanol, ethanol, and ethylene glycol. Symbols: experimental band integral BI(364,-430) taken over the ESA2 band from Figure 5. Solid curves: monoexponential fits.

better agreement between the solvation correlation function $C(t)$ and the transient Stokes shift data in these solvents (see Figure 6b,c).

V. Reorganization Energies and Absorption Band Shape

Now we make use of the parameters $\Delta\nu_S$ and $\nu_{SE}(0)$ which were obtained from fits of the transient Stokes shift data $\nu_{SE}(t)$ (Figure 6) in order to analyze the absorption spectrum of betaine-30. Usually, the absorption band shape is empirically described with a log-normal distribution. Its asymmetric profile reflects the Franck−Condon progression of high frequency solute modes, whereas the width of the band is determined by both solute and solvent contributions. The exact analytic form of the log-normal parameters is generally rather complex[15] but can be simplified when (i) only a few vibrational modes are optically active and (ii) solvent broadening is sufficiently large to smear out high-frequency spectral structure. In this case, as shown by Kjaer and Ulstrup,[15] the absorption band near the maximum can be described by a Gaussian with its peak ν_A and width Γ_A expressed as

$$\nu_A = \Delta F_0 + \lambda_i + \lambda_s \tag{6a}$$

$$\Gamma_A^2 = \sum_j \Gamma_j^2 \tag{6b}$$

where ΔF_0 is the free energy gap and λ_i and λ_S denote intramolecular and solvent reorganization energies. Figure 1b shows Gaussian fits of the absorption spectra of betaine-30 in acetonitrile and chloroform. Typically, when the peak frequency is fixed at the absorption maximum, the fitted width deviates from the experimental one by less than 5% which justifies the above simplified approach.

The widths Γ_j are related to reorganization energies λ_j as

$$\Gamma_j = 2.355\sqrt{\lambda_j \Omega_j \coth(\Omega_j/2kT)} \tag{7a}$$

where Ω_j is the frequency of the relevant mode. For low and high frequencies, eq 7a reads

$$\Gamma_l = 2.355\sqrt{2\lambda_l kT}, \quad \Omega_l \ll kT \tag{7b}$$

$$\Gamma_h = 1.665\sqrt{2\lambda_h \Omega_h}, \quad \Omega_h \gg kT \tag{7c}$$

We further assume three contributions to the absorption width. One comes from a high-frequency intramolecular mode with $\Omega_h = 1350$ cm.$^{-1}$ This mode is seen in the early transient spectra (Figures 2a, 3a, and 4a) as a pronounced Raman signal. The reorganization energy λ_h and the dimensionless displacement Δ_h for this mode are directly obtained from the detuning $\Delta\nu_h$ of the time-zero SE peak from the absorption maximum

$$\Delta\nu_h = 2\lambda_h = \nu_A - \nu_{SE}(0), \quad \Delta_h = \sqrt{2\lambda_h/\Omega_h} \tag{8}$$

where $\nu_{SE}(0)$ is given by the fits shown in Figure 6. In ethanol, green and red excitation allow two estimates of the high-frequency reorganization energy. The first, calculated with eq 8 for 532 nm excitation, gives $\lambda_h = 1870$ cm.$^{-1}$ The second estimate is obtained as the detuning of $\nu_{SE}(0)$ from the red excitation frequency (15 800 cm^{-1}), which in this case is close to the 0−0 transition. This gives a somewhat larger value of 2190 cm^{-1}, probably because the pump still excites a fraction of molecules with excess vibrational energy.

The low-frequency contributions come from solvation and solute intramolecular relaxation. The solute contribution is required to adjust the full absorption width according to the condition

$$\Gamma_A = \sqrt{\Gamma_h^2 + \Gamma_S^2 + \Gamma_c^2} \tag{9}$$

We call this contribution Γ_c "conformational" and suggest that it is related to rotational motion of the phenyl rings. When Γ_S and Γ_h are known, Γ_c is calculated from eq 9. This contribution to the absorption bandwidth is quite substantial in all solvents, being 2100 cm^{-1} in acetonitrile and chloroform and of 1700 cm^{-1} in alcohols.

The solvation contribution $\Delta\nu_S$, and hence Γ_S, is obtained from the same fits (Figure 6) as $\Delta\nu_h$. Additionally, an independent estimate of Γ_S can be derived from the time-zero SE spectra which originate from conformations selected by the excitation pulse. Because the conformational relaxation is assumed to be slow, the early SE spectra are not broadened by the latter process and the corresponding width is calculated as[43]

$$\Gamma_{SE}(0) = \sqrt{\Gamma_h^2 + \Gamma_S^2} \tag{10}$$

For acetonitrile and ethanol, for example, eq 10 gives $\Gamma_{SE}(0) =$ 3910 and 4470 cm,$^{-1}$ respectively, in satisfactory agreement (within 10−15%) with the experimental values of Table 1. Nonetheless, because the observed widths are smaller than the

TABLE 3: Free Energy Gap ΔF_0, Spectral Shifts $\Delta\nu$, and Reorganization Energies λ and Their Contributions to the Absorption Band Width Γ_A[a]

solvent	ΔF_o	Γ_A	Γ_S	$\Delta\nu_S$	λ_S	Γ_h	$\Delta\nu_h$	λ_h	Ω_h	Δ_h	Γ_c	λ_c
acetonitrile	10 940	4450	2150	4000	2000	3270	2860	1430	1350	1.46	2120	1940
chloroform	10 720	3590	1380	1650	830	2560	1750	880	1350	1.14	2100	1910
methanol	13 290	5100	2450	5200	2600	4170	4640	2320	1350	1.85	1620	1130
ethanol	12 290	4800	2440	5150	2580	3740	3730	1870	1350	1.66	1760	1340
ethyl. glyc.	13 750	5230	2100	3800	1900	4450	5300	2650	1350	1.98	1770	1350

[a] All values in units of cm^{-1} (1 kcal/mol = 350 cm^{-1}). $\Delta F_0 = \nu_A - \lambda_S - \lambda_h - \lambda_c$. $\Gamma_A = \sqrt{\Gamma_S^2+\Gamma_h^2+\Gamma_c^2}$. Subscripts s, h, and l denote solvation, high frequency and low frequency (conformational) intramolecular contributions, respectively. $\Gamma_{S,c} = 2.355(kT\Delta\nu_{S,c})^{1/2}$ (kT = 208.5 cm^{-1}), and $\Gamma_h = 1.665(\Omega_h\Delta\nu_h)^{1/2}$. $\Delta\nu_j$ and $\lambda_j = \Delta\nu_j/2$ are spectral shifts and reorganization energies. $\Delta\nu_h = \nu_A\nu_{SE}(0)$, and $\Delta_h = (\Delta\nu_h/\Omega_h)^{1/2}$. The accuracy for λ_i is ±10%.

calculated ones, this may indicate an overestimate (again within 10%) in solvation reorganization energies.

Table 3 summarizes our results concerning reorganization energies and associated spectral broadening. The first column shows also the free energy gap $\Delta F_0 = (\nu_A - \lambda_h - \lambda_S - \lambda_c)$.

VI. Discussion

It follows from the above analysis that the photoinduced evolution of betaine-30 should be depicted, rather than by Scheme 1, as

$$(D^+A^-)_g \xrightarrow{h\nu} (DA)_e^{FC} \xrightarrow[\text{solvation}]{\text{rhfv iET}} (DA)_e^{r} \xrightarrow{\text{bET}} (D^+A^-)_g^{hot} \qquad (11)$$

where D and A are the donor and acceptor of charge, respectively. Photoexcitation $h\nu$ transfers the molecule from the ground-state g to the excited Franck−Condon (superscript FC) state e. Relaxation of high-frequency vibrational modes (rhfv) proceeds just afterward on a 10 fs time scale. This relaxation is not resolved in our experiments but recognized as an initial detuning of the early SE spectra from the absorption maximum. Then two processes take place almost simultaneously: solvation and conformational rearrangement of the solute. The latter is related to a change of the dipole moment; therefore, we call it intramolecular ET. A characteristic time scale here is ∼100 fs depending on the solvent. In acetonitrile and methanol, iET adiabatically follows solvent relaxation; in ethanol and chloroform, it is slower (Table 2), which may be due to insufficient driving force created by solvation. Conformational rearrangement can be viewed as relaxation of low-frequency vibrational modes in the excited state.

What modes are responsible for iET remain unclear; this interesting problem requires further work. Intramolecular ET is experimentally recognized as a decrease of the oscillator strength for SE and as a synchronous increase of the oscillator strength for DSA. Internal conversion or bET proceeds with a 1−10 ps time constant from the conformationally relaxed (superscript r) excited state. Because the optical properties of this state differ from those of the ground state, the rate of bET cannot be related in a simple way with the steady-state absorption spectra.

One of the essential points in our study concerns the insight which is possible with broad spectral detection. By monitoring simultaneously the evolution of excited state absorption and stimulated emission, we find that they decay with different time constants and, thus, distinguish between iET and bET. Recently, we studied other probes, *p*-nitroaniline (PNA) and dimethylamino-*p*-nitroaniline (DPNA),[40,41] which show similar characteristic behavior: intramolecular and back ET in PNA and DPNA are also exposed via a fast decay of SE and a slower decay of ESA, respectively. It seems that the discovered different sensitivity of SE and ESA to intramolecular rearrangements may be general for many nonfluorescing compounds with a benzene moiety.

Another important point concerns our approach for determining reorganization energies from early spectral shifts. We assumed that the *early* evolution is weakly affected by iET and, therefore, proceeds as for an ideal solvatochromic probe. With this assumption, we extracted ground-state solvation reorganization energies and characterized various intra- and intermolecular contributions to the absorption line width. Note that the measured width $\Gamma_{SE}(0)$ of the time-zero SE spectra in acetonitrile, chloroform, and ethanol is in agreement with solvation reorganization energies obtained in this way, which supports the above assumption.

Solvation correlation functions $C(t)$ merit a special remark. We used them for comparison with iET dynamics and for the fits of spectral shifts. It is worth noting that femtosecond solvation measurements which are reliable for our purposes have become available only recently,[30,31,34−36,39,44] mainly owing to work by Maroncelli's group.[30,31] A problem here is that any solvatochromic probe may exhibit "slow" excited-state intramolecular dynamics overlaid with solvation. Nonetheless, it has been shown that $C(t)$ measured with coumarin 153[30] and aminonitrofluorene[35] in acetonitrile are in reasonable agreement with each other and with dielectric and far-infrared data.[45,46] Thus, although for other solvents $C(t)$ may still have to be corrected, it seems to be well established for acetonitrile. We therefore paid special attention to this solvent which can be considered as a benchmark for comparison both with the results by other workers and with our own measurements in different solvents.

Let us discuss solvation reorganization energies of betaine-30 first. Our result for acetonitrile (2000 ± 200 cm^{-1}) falls between the estimates by Kjaer and Ulstrup[15] (1660 cm^{-1}) and by Barbara's group[4] (2220 cm^{-1}). The value of 2000 cm^{-1} is also consistent with a prediction[3,19] from simple dielectric continuum theory

$$\lambda_S = \frac{(\mu_g - \mu_e^{FC})^2}{hcR^3} f(\epsilon,n) \qquad (12)$$

where R is the solute cavity radius and $\mu_{g,e}^{FC}$ the dipole moment in the ground and Franck−Condon excited states. The solvent function f depends on susceptibility ϵ and refractive index n and is given by[3] $f_1(\epsilon,n) = [(\epsilon - 1)/(2\epsilon + 1) - (n^2 - 1)/(2n^2 + 1)]$ or by[19] $f_2(\epsilon,n) = [(\epsilon - 1)/(\epsilon + 2) - (n^2 - 1)/(n^2 + 2)]$ differing for $\epsilon \gg 1$ by a factor of 2. Taking $(\mu_g - \mu_e^{FC}) \approx 20$ D[22,18,19,3] and λ_S = 2000 cm^{-1}, one obtains R_1 = 6.7 Å or R_2 = 8.9 Å, respectively, in excellent agreement with calculations of betaine-30 molecular geometry.[19,47]

Recent computational studies of betaine-30 in acetonitrile by Mente and Maroncelli[19] and by Lobaugh and Rossky[18] report

the reorganization energy as $\lambda_S = 2570$ and 3625 cm,$^{-1}$ respectively. A much larger value of $\lambda_S \approx 6000$ cm^{-1} was derived by Zong and McHale[8] from resonance Raman measurements. We briefly comment on the last result. First, $\lambda_S \approx 6000$ cm^{-1} is inconsistent with the absorption spectrum which is too narrow to accommodate such energy. Therefore, the authors[8] were forced to assume strong violation of the linear response. The latter is, however, unlikely because all solvation dynamics studies,[30−39] including those with strongly solvatochromic probes,[35,39] are in agreement with linear response predictions. Furthermore, the observables in Raman spectroscopy are cross sections and excitation profiles which are affected by the rate of excited-state electronic dephasing. To derive λ_S, Zong and McHale assumed implicitly that dephasing is governed solely by solvent relaxation. Our results show that there exist other sources of ultrafast dephasing, namely, vibrational relaxation of high-frequency modes and iET. In particular, the rate of vibrational relaxation must show a pronounced dependence on the excitation wavelength, becoming very small when 0−0 transition is excited. Thus, the Raman excitation profiles must be corrected for this effect. Note in this regard that, the ability of resonance Raman spectroscopy to correctly reproduce solvation dynamics has not been checked so far. This could be done by measuring reasonably "well-behaved" molecules such as coumarin 153[30,31] or aminonitrofluorene[35] (the latter probe is especially suitable because of its relatively low fluorescence yield).

Last, consider intramolecular reorganization energies represented in Table 3 by high frequency (Ω_h, λ_h) and low frequency (λ_c) modes. It is seen that λ_h and, hence, the displacement Δ_h and the corresponding Franck−Condon factors strongly depend both on solvent polarity and on the ability for hydrogen bonding. When going from chloroform to acetonitrile, λ_h grows from 880 to 1430 cm^{-1} and further increases in methanol to a value of 2320 cm.$^{-1}$ This behavior suggests a solvent dependence of the solute equilibrium geometry in the ground state. Low-frequency reorganization energies λ_c then reflect a distribution of these geometries. Therefore the solvatochromic shift of the absorption band contains substantial intramolecular contributions which are in turn solvent dependent. We believe that solvatochromism of betaine-30 cannot be modeled without accounting for intramolecular degrees of freedom.

In conclusion, we hope that the presented experimental results will stimulate theoretical work to model the excited-state dynamics of this betaine dye.

Acknowledgment. We gratefully acknowledge the Volkswagen Stiftung and the Deutsche Forschungsgemeischaft for financial support.

References and Notes

(1) Reichardt, C. *Chem. Rev.* **1994**, *94*, 2319.
(2) Reicnardt, C. *Solvents and Solvent Effects in Organic Chemistry*; Weinheim, 1988.
(3) Liptay, W.; Dumbacher, B.; Weisenberger, H. *Z. Naturforsch.* **1968**, *23a*, 1601.
(4) Walker, G. C.; Akesson, E.; Jonson, A. E.; Levinger, N. E.; Barbara, P. F. *J. Phys. Chem.* **1992**, *96*, 3728.
(5) Reid, P. J.; Barbara, P. F. *J. Phys. Chem.* **1995**, *99*, 3554.
(6) Reid, P. J.; Simson, A.; Jarzeba, W.; Schlief, R. E.; Johnson, A. E.; Barbara, P. F. *Chem. Phys. Lett.* **1994**, *229*, 93.
(7) A comprehensive review of betaine-30 is given in ref 19.
(8) Zong, Y.; McHale, J. L. *J. Chem. Phys.* **1997**, *106*, 4963; *107*, 2920.
(9) Hogiu, S.; Wernke, W.; Pfeiffer, M.; Elsaesser, T. *Chem. Phys. Lett.* **1999**, *312*, 407.
(10) (a) Hogiu, S.; Dreyer, J.; Pfeiffer, M.; Brezinka, K.-W.; Wernke, W. *J. Raman Spetrosc.* **2000**, *31*, 797. (b) Hogiu, S.; Wernke, W.; Pfeiffer, M.; Dreyer, J.; Elsaesser, T. *J. Chem. Phys.* **2000**, *113*, 1587.
(11) Sumi, H.; Marcus, R. A. *J. Chem. Phys.* **1986**, *84*, 4894.
(12) Jortner, J.; Bixon. M. *J. Chem. Phys.* **1988**, *88*, 167.
(13) Fuchs, C.; Schreiber, M. *J. Chem. Phys.* **1996**, *105*, 1023.
(14) Gayathri, N.; Bagchi, B. *J. Chim. Phys.* **1996**, *93*, 1652.
(15) Kjaer, A. M.; Ulstrup, J. *J. Am. Chem. Soc.* **1987**, *109*, 1934.
(16) Perng, B.-C.; Newton, M. D.; Raineri, F. O.; Friedman, H. L. *J. Chem. Phys.* **1996**, *104*, 7177.
(17) Matyushov, D. V.; Schmid, R.; Ladanyi, B. M. *J. Phys. Chem. B*, **1997**, *101*, 1035.
(18) Lobaugh, J.; Rossky, P. J. *J. Phys. Chem. A* **1999**, *103*, 9432; **2000**, *104*, 899.
(19) Mente, S. R.; Maroncelli, M. *J. Phys. Chem. B* **1999**, *103*, 7704.
(20) Kulinowski, K.; Gould, I. R.; Myers, A. B. *J. Phys. Chem.* **1995**, *99*, 9017.
(21) Alencastro, R. B.; Neto, J. D. D. M.; Zerner, M. C. *Int. J. Quantum Chem. Quantum Chem. Symp.* **1994**, *28*, 361.
(22) Lipinski, J.; Bartkoviak, W. *J. Phys. Chem. A* **1997**, *101*, 2159.
(23) Bartkoviak, W.; Lipinski, J. *J. Phys. Chem. A* **1998**, *102*, 5236.
(24) Kovalenko, S. A.; Dobryakov, A. L.; Ruthmann, J.; Ernsting, N. P. *Phys. Rev. A* **1999**, *59*, 2369.
(25) Kovalenko, S. A.; Ernsting, N. P.; Ruthmann, J. *Chem. Phys. Lett.* **1996**, *258*, 445.
(26) Lochschmidt, A.; Eilers-König, N.; Heineking, N.; Ernsting, N. P. *J. Phys. Chem. A* **1999**, *103*, 1776.
(27) Loring, R. F.; Yan, Y. J.; Mukamel, S. *J. Chem. Phys.* **1987**, *87*, 5840.
(28) Kang, T. J.; Yu, J.; Berg, M. *J. Chem. Phys.* **1991**, *94*, 2413.
(29) Yan, Y. J.; Mukamel, S. *J. Chem. Phys.* **1987**, *86*, 6085.
(30) Horng, M. L.; Gardecki, J. A.; Papazyan, A.; Maroncelli, M. *J. Phys. Chem.* **1995**, *99*, 17311.
(31) Reynolds, L.; Gardecki, J. A.; Frankland, S. J. V.; Horng, M. L.; Maroncelli, M. *J. Phys. Chem.* **1996**, *100*, 10337.
(32) Kovalenko, S. A.; Ruthmann, J.; Ernsting, N. P. *J. Chem. Phys.* **1998**, *109*, 1894.
(33) Maroncelli, M. *J. Chem. Phys.* **1991**, *94*, 2084.
(34) Castner, E. W., Jr.; Maroncelli M. *J. Mol. Liq.* **1998**, *77*, 1.
(35) Ruthmann, J.; Kovalenko, S. A.; Ernsting, N. P.; Ouw, D. *J. Chem. Phys.* **1998**, *109*, 5466.
(36) Kovalenko, S. A.; Senyushkina, T. A.; Ernsting, N. P.; Hennig, H.; Laurent, T. F.; Frese, J. *Phys. Chem. Chem. Phys.* **2000**, submitted for publication.
(37) Hsu, C.-P.; Song, X.; Marcus, R. A. *J. Phys. Chem. B* **1997**, *101*, 2546.
(38) Hsu, C.-P.; Georgievskii, Y.; Marcus, R. A. *J. Phys. Chem. A* **1998**, *102*, 2658.
(39) Kovalenko, S. A.; Senyushkina, T. A.; Ernsting, N. P. Manuscript in preparation.
(40) Kovalenko, S. A.; Schanz, R.; Farztdinov, V. M.; Hennig, H.; Ernsting, N. P. *Chem. Phys. Lett.* **2000**, *323*, 312.
(41) Farztdinov, V. M.; Kovalenko, S. A.; Schanz, R.; Ernsting, N. P. *J. Phys. Chem. A* **2000**, *104*, 11486.
(42) Contrary to the partial band integral, the full band integral is insensitive to temperature. When internal conversion is complete, the full band integral is identically zero. See ref 40.
(43) The solvation broadening proceeds on a time scale $\tau \approx \tau_S/5 \approx 20$ fs (see ref 27). Therefore, it must be included in the width of the time-zero SE spectra.
(44) Gustavsson, T.; Cassara, L.; Gulbinas, V.; Gurzadyan, G.; Mialocq, J.-C.; Pommeret, S.; Sorgius, M.; Meulen v. d., P. *J. Phys. Chem. A* **1998**, *102*, 4229.
(45) Barthel, K.; Bachhuber, K.; Buchner, R.; Gill, J. B.; Kleebauer, M. *Chem. Phys. Lett.* **1990**, *167*, 62.
(46) Ohba, T.; Ikawa, S. *Mol. Phys.* **1991**, *73*, 985.
(47) Zong and McHale[8] claimed that the continuum theory gives for betaine-30 the solvation reorganization energy of 200 cm^{-1}. This underestimate comes from an inappropriate value of $R = 14$ Å used.